JOC The Journal of Organic Chemistry

Article

pubs.acs.org/joc

Substituent and Solvent Effects on the Stability of *N*-Heterocyclic Carbene Complexes with CO_2

Derek M. Denning and Daniel E. Falvey*

Department of Chemistry and Biochemistry, University of Maryland, College Park, Maryland 20742, United States

Supporting Information

ABSTRACT: Carbon dioxide forms covalent complexes with N-heterocyclic carbenes. These complexes are of interest in catalysis as well as for their potential use in various carbon capture and storage strategies. A previous report showed that the stability of one such complex, *N*,*N*-dimethylimidazolium 2-carboxylate, was remarkably sensitive to solvent polarity. Polar environments lead to a kinetically stronger, shorter, and more polar bond between the carbene and CO_2. The current study shows that this solvent effect is general across a wide range of NHC complexes with CO_2. Computational modeling at the DFT level shows that the lability of these bonds can be controlled by steric pressure due to substituents on the heteroatoms flanking the carbene center, as well as inductive electronic effects from substituents on the C4 and C5 positions. Moreover, a strong correlation between the gas-phase NHC−CO_2 bond distance and the Gibbs free energy barrier for decarboxylation is demonstrated.

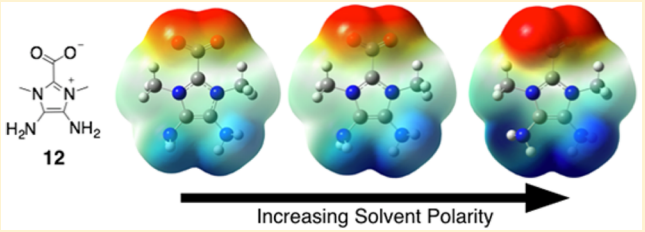

INTRODUCTION

Carbon dioxide (CO_2) emission from anthropogenic sources is driving concerns over climate change, as this greenhouse gas has reached atmospheric concentration levels never observed before.[1] Current efforts aimed at the mitigation of this gas involve developing materials and reagents capable of reversible binding to CO_2 in a strategy known as carbon capture and storage (CCS).[2,3] The sequestration of carbon dioxide is currently being explored using various agents, including polyamine adsorbent materials,[4−7] ionic liquids,[8,9] frustrated Lewis pairs,[10,11] and metal-organic frameworks.[12] While the aforementioned materials exhibit enhanced binding to CO_2, it is also important that this binding be weak enough to permit the conversion of this gas into other usable chemicals and/or fuels as part of a broader carbon capture and utilization process (CCU). Continuous efforts have demonstrated the inclusion of CO_2 into various functional groups including cyclic carbonates/carbamates,[13,14] the methylation of amines,[15] and the formation of amides[16] and carboxylic acids.[17] Carbon dioxide can also be electrochemically reduced to afford products such as carbon monoxide and formic acid.[18,19] However, an important goal with the aforementioned transformation processes is that the energy input required for conversion of CO_2 should be independent from CO_2-emitting sources. Thus, our group is interested in developing reagents that can facilitate photochemical reduction of CO_2.

Our current interest is focused on the use of *N*-heterocyclic carbenes (NHCs), which are defined as neutral compounds consisting of a carbene carbon center that is adjacent to at least one nitrogen atom, generally existing within a ring structure. Previous reports have established the reactivity of these species with CO_2, forming stable zwitterionic *N*-heterocyclic 2-carboxylates (NHC−CO_2),[20−22] Several groups have investigated the stability of such complexes. For example, experiments by Louie et al.[25] showed that sterically demanding substituents in the 1- and 3-positions leads to more facile decarboxylation. Ajitha and Suresh examined a variety of such complexes by DFT and found a correlation between the strength of CO_2 binding and the minimum electrostatic potential calculated for the formal lone pair on the NHC.[23] An additional consideration is the effect of the solvent on rates of decarboxylation. Several reports illustrated a wide range of stability for these species in mixed solvents of varying polarity[24,25] (as defined by the $E_T(30)$ solvent polarity scale).[26,27] Polar solvents stabilize these compounds by favoring the formation of the zwitterionic adducts, while less polar solvents favor decarboxylation products (Scheme 1).

A related study demonstrated that one such adduct, 1,3-dimethylimidazolium carboxylate (**2**), can be photochemically reduced, effecting a net conversion of CO_2 to formic and oxalic acid.[28] While this result is promising, it would be desirable to develop this reaction into a catalytic process. To do so will require optimization of several aspects of the reaction, including the strength of the NHC−CO_2 bond; weak affinity will prevent capture and photoreduction, but binding that is too strong is likely to inhibit turnover of the reduced intermediate(s). The present study was undertaken with the goal of validating simple computational methods that would allow a wide range of NHCs to be rapidly screened for their CO_2 affinity by examining 26 NHC−CO_2 models with various substituent effects (Figure 1). In addition, given the strong solvent

Received: November 16, 2016
Published: January 9, 2017

DOI: 10.1021/acs.joc.6b02755
J. Org. Chem. 2017, 82, 1552−1557

Scheme 1. Stability and Photochemical Reduction of NHC−CO_2

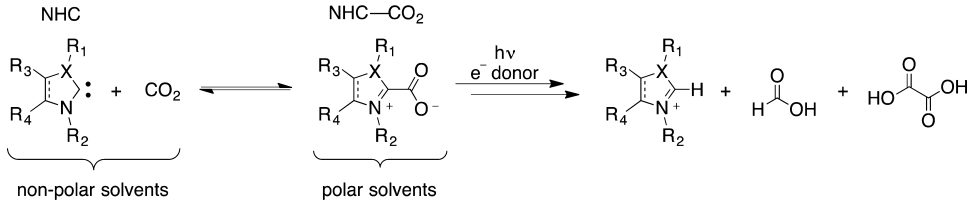

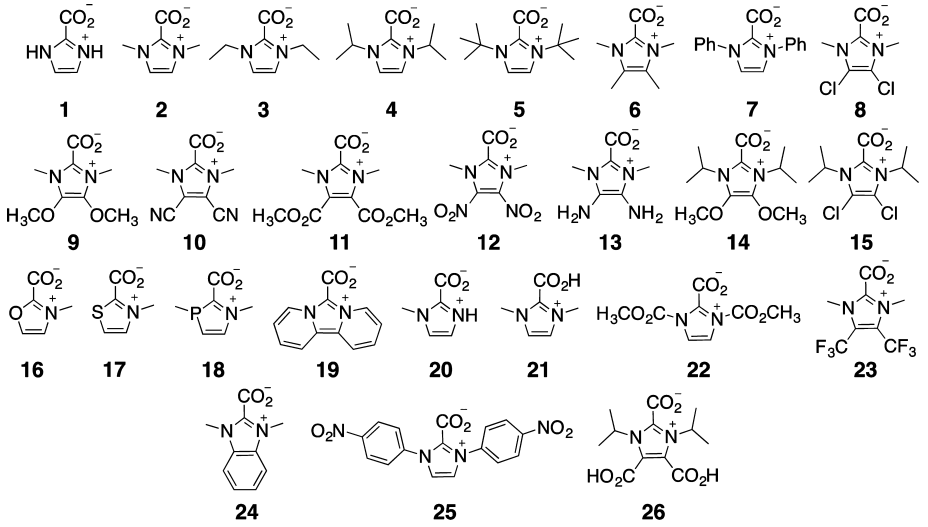

Figure 1. The 26 NHC−CO_2 complexes examined in this study.

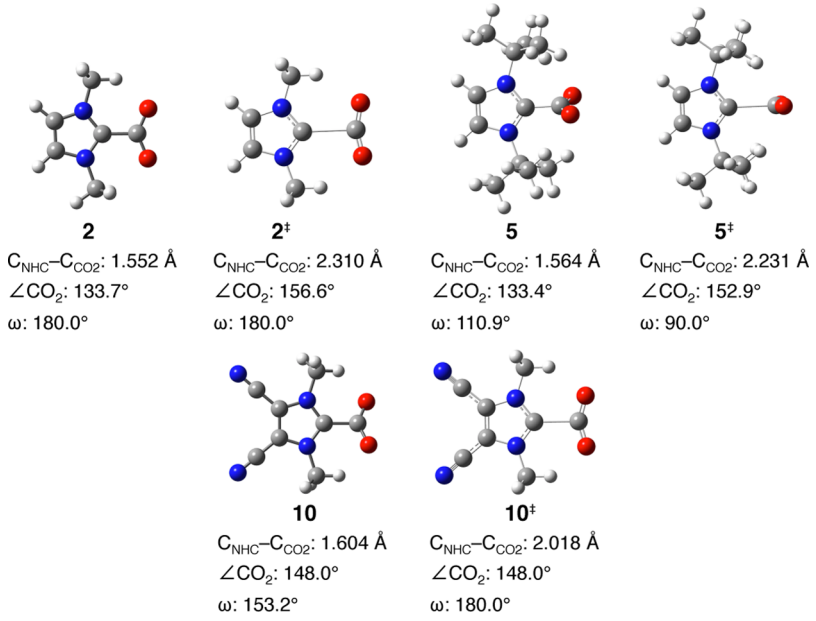

Figure 2. Selected geometries of NHC−CO_2 **2**, **5**, and **10**, along with their corresponding transition states **2**‡, **5**‡, and **10**‡, using DFT-B3LYP/6-31G(d,p) in the gas phase.

dependence observed for **2**, it was of particular interest to characterize solvent effects on decarboxylation rates.

■ COMPUTATIONAL METHODS

The calculations described in this paper were carried out using Gaussian09.[29] NHC−CO_2 compounds were optimized using density functional theory (DFT) at the B3LYP/6-31G(d,p) level.[30,31] Transition-state geometries were optimized by QST3 following a scan calculation of the C_{NHC}−C_{CO2} bond (30−40 scans in 0.05 Å increments). In cases where the effects of solvent were to be modeled, Truhlar's implicit solvation model (SMD) was used.[32] This combination of basis set, functional, and solvent model was chosen in light of a previous study, where it was found to give excellent agreement with experimentally determined Gibbs free energy barriers for the decarboxylation process.[24] However, other functionals (M11,[33] M062X,[34] B3PW91[35]) provided similar trends when the geometry was examined under various solvation conditions. Frequency calculations were carried out and used to verify that the stationary points were

DOI: 10.1021/acs.joc.6b02755
J. Org. Chem. 2017, 82, 1552−1557

either local minima (0 imaginary frequencies) or transition states (1 imaginary frequency).

RESULTS AND DISCUSSION

Results from the current study establish the following.

(1) The kinetic stability of NHC−CO_2 binding is inversely correlated with the corresponding C_{NHC}−C_{CO2} bond distance. The latter quantity is easily computed using inexpensive and readily available DFT methods with implicit solvation models (e.g., SMD-B3LYP/6-31G(d,p)).

(2) Binding of CO_2 can be controlled by both steric and electronic effects: inductive electron acceptors on the backbone carbons and sterically demanding substituents on the nitrogens tend to reduce the binding affinity, whereas inductive donors and/or small N substituents tend to increase the affinity.

(3) The remarkable solvent dependence on CO_2 binding shown experimentally for **2** (i.e., strong in polar solvents and weak in nonpolar media) is generally true for a wide variety of NHC derivatives.

(4) The sensitivity of the C_{NHC}−C_{CO2} bond to solvation is related to the length of the bond calculated in the gas phase. Weaker C_{NHC}−C_{CO2} bonds (gas phase) are more sensitive to polarity. However, sterically demanding substituents on the nitrogens can cause the CO_2 group to rotate out of coplanarity with the imidazolium ring. In those cases, the sensitivity to solvent polarity diminishes.

Decarboxylation Barrier and Substituent Effects. Shown in Figure 2 are detailed geometries of NHC−CO_2 species **2, 5**, and **10**. Of note is the bond distance between the C2 carbon on the NHC group and the carbon on the carboxyl group. These bond distances are long relative to what is typical for a C_{sp^2}−C_{sp^2} single bond (1.46 Å for 1,3-butadiene).[36] In the case of **2**, the distance is 1.55 Å, but for the electron-deficient 4,5-dicyano derivative **10** it is 1.60 Å. The O−C−O angle in the carboxyl group also reflects the extent of NHC−CO_2 interaction. These were found to range from 138.6° for weaker complexes such as **22** to 122.8° for more tightly bound examples such as **21**. In the simplest examples, such as **1** and **16**, the carboxylate group maintains conjugation with the NHC ring by adopting a coplanar geometry, or nearly so (ω = 180°). However, in cases where there is significant steric pressure from substituents on the flanking heteroatoms, the carboxylate group rotates out of plane. For example, in the case of the 1,3-di-*tert*-butyl system **5**, the carboxylate group is nearly orthogonal to the ring (ω = 110.9°).

As inferred in the previous study, the increased NHC−CO_2 bond distance in the transition state is accompanied by decreasing charge separation. Figure 3 compares the electrostatic potential distribution between compounds **10** and **13** and their corresponding decarboxylation transition states, illustrating the decreased charge separation in this case. This decrease in charge separation appears to be consistent across the series of transition states examined. Table 1 gives dipole moments for selected complexes and their corresponding transition states. In each case the dipole moment was found to decrease when the transition state was compared with the corresponding NHC−CO_2 derivative.

The wide variation of NHC−CO_2 bond distances and O−C−O bond angles with substituents suggests that the several examples differ in the degree to which the C−C bond is formed. It seems reasonable to expect that these parameters would follow, and perhaps predict, the lability of the bond. In order to understand the relationship of geometry to the kinetic

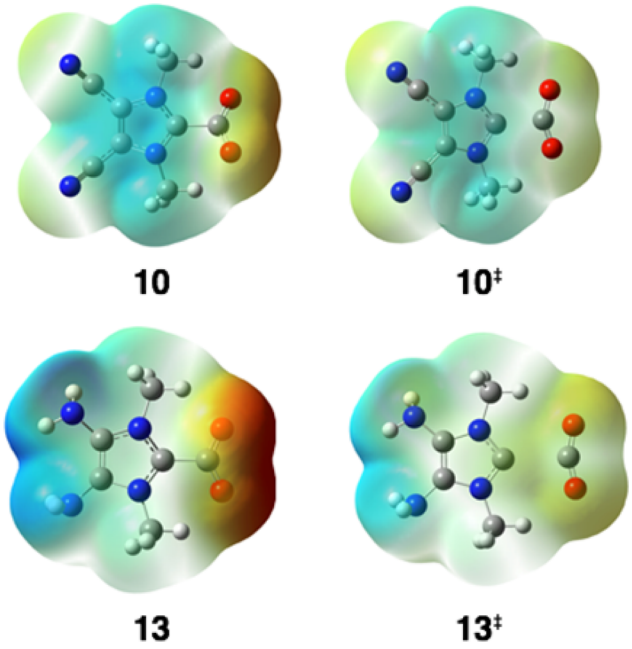

Figure 3. Structures derived from DFT optimizations in the gas phase on NHC−CO_2 species **10** and **13** and their corresponding transition states. The shaded isosurfaces are representations of the molecular electrostatic potential, where dark blue denotes positive charge density (+0.092 e/Å^3) and dark red denotes negative charge density (−0.092 e/Å^3).

stability of NHC−CO_2 species, gas-phase barriers to decarboxylation and transition states for the decarboxylation process were located and characterized (Table 1). Frequency calculations then provided Gibbs free energy differences between the transition states and the reactants ($\Delta G^{\ddagger}$, kcal/mol, 298 K, 1 atm, gas phase). In most cases, a weakly bound complex between CO_2 and the NHC was found immediately after the transition state and could be characterized as a local minimum. The ΔG° values reported in Figure 4 and Table 1 represent the Gibbs free energy difference (kcal/mol, 298 K, 1 atm, gas phase) between the NHC−CO_2 and said weakly bound complex. As is apparent from Table 1, the decarboxylation reactions range from weakly endergonic to weakly exergonic. More significantly, the free energy barriers to decarboxylation show a good correlation with the driving force for decarboxylation (Figure 4). Excluded from the fit was the di-N-*tert*-butyl derivative **5**. In this example, steric pressures force the CO_2 group to rotate out of plane, in both the reactant and the transition state.

The wide variation in NHC−CO_2 bond distances further suggested that this parameter might reflect that strength of the NHC−CO_2 bond and consequently its kinetic lability. The plot shown in Figure 4 confirms this relationship by illustrating a linear connection between the bond length and the free energy of activation.

Interestingly, compounds **5** and **9** exhibit similar calculated gas-phase bond distances and barriers to decarboxylation, even though their substituents are widely different. The large *tert*-butyl substituents on **5** cause the carboxylate group to rotate out of conjugation with the heterocyclic ring, as evidenced by the dihedral angle shown in Figure 2. While the bond length for **9** is similar, the dihedral angle exhibits a twist toward planarity in comparison to that in **5**, suggesting a large role that the methoxy substituents have for the electronic effects to the

DOI: 10.1021/acs.joc.6b02755
J. Org. Chem. 2017, 82, 1552−1557

Table 1. Selected Geometric Parameters, Dipole Moments, and Free Energy Barriers to Decarboxylation for Various NHC–CO_2 Species in the Gas Phase

NHC–CO_2	C_{NHC}–C_{CO2} (Å)	D (D)	C_{NHC}–$C_{CO2}^{‡}$ (Å)	$D^{‡}$ (D)	ΔC_{NHC}–C_{CO2}	dihedral angle (deg)	$\Delta G^{‡}$ (kcal/mol)	ΔG° (kcal/mol)
3	1.570	8.72	2.345	4.75	0.775	169.7	6.02	3.23
5	1.564	7.95	2.231	5.14	0.667	110.9	6.42	−0.09
8	1.598	7.20	2.155	3.82	0.557	159.6	3.35	−1.46
9	1.579	10.9	2.327	6.09	0.748	160.6	6.00	3.60
10	1.604	2.88	2.018	0.51	0.414	153.1	1.47	−5.88
16	1.613	10.3	1.980	8.30	0.367	180.0	1.05	−6.33
17	1.585	9.85	2.071	7.37	0.486	180.0	2.62	−3.63
19	1.553	10.3	2.266	5.65	0.713	180.0	7.86	4.84
23	1.592	5.87	2.087	3.01	0.495	144.2	2.42	−4.17

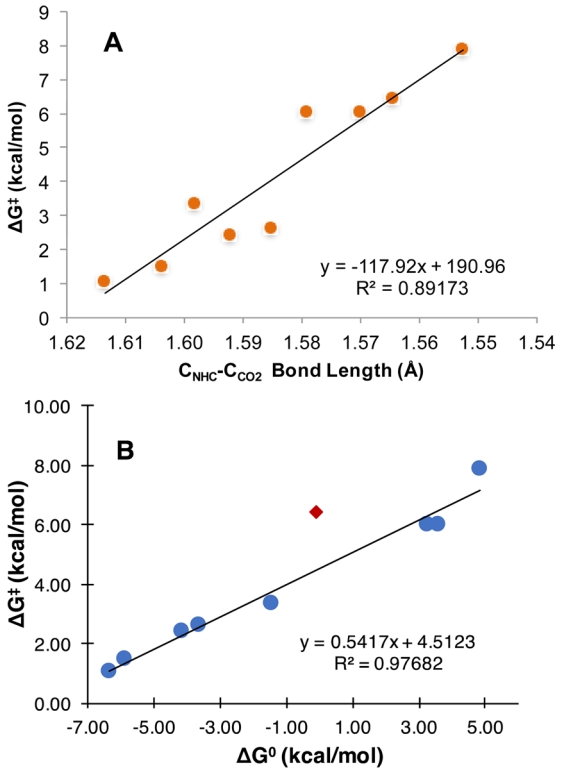

Figure 4. (A) Correlation of C_{NHC}–C_{CO2} bond length and the free energy barrier to decarboxylation for select NHC–CO_2 species in the gas phase. (B) Linear free energy relationship between the decarboxylation barrier and the driving force for decarboxylation. The red diamond point represents the sterically hindered complex **5** and was not included in the fit.

C_{NHC}–C_{CO2} bond length. The methyl groups on **9** allow the carboxylate moiety to get closer to the heterocyclic ring, but the mesomeric effects of the ring substituents contribute to the lengthening of the C_{NHC}–C_{CO2} bond, resulting in similar free energy barriers to decarboxylation for **5** and **9**. Thus, it appears that calculated bond distances of the C_{NHC}–C_{CO2} bond could serve as a model for predicting the stability of N-heterocyclic 2-carboxylates relative to their decarboxylated products in various solvents.

In agreement with previous reports,[23,37] it is found here that increasing the steric pressures on the flanking heteroatoms leads to an increase in the aforementioned bond distance. Compound **2** (methyl groups) has a calculated bond distance of 1.522 Å in water in comparison to that of 1.538 Å (*tert*-butyl groups) for compound **5**. While large bulky substituents have a profound effect on the C_{NHC}–C_{CO2} bond distance, electronic effects can have a similar influence without the sterically encumbered heteroatom substituents.

Valence bond representations of **2** allow for formal positive charge on N1, N3, or C2 but not directly on C4 or C5 (the backbone carbon atoms). This suggests that the effect of C4 and C5 substituents should be primarily inductive, rather than through resonance. Free energy barriers for decarboxylation ($\Delta G^{‡}$) were calculated for the examples shown in Figure 4. These complexes all have methyl groups on N1 and N3 and thus have similar steric effects on the barriers. The inductive electronic effects vary from two electron-donating alkyl groups to strongly withdrawing nitro groups. As expected, inductive electron-withdrawing groups reduce the decarboxylation barrier in comparison to the unsubstituted case. Figure 5 compares the

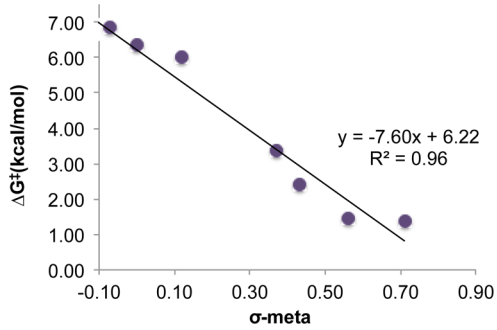

Figure 5. Linear free energy relationship between predicted decarboxylation rates and the Hammett meta parameter.

decarboxylation barriers and illustrates a negative correlation with the Hammett substituent parameter σ_{meta}, having ρ = −7.60. Attempts to correlate these barriers with σ_{para} or other resonance-based substituent parameters provided correlations that were significantly weaker.[38]

Solvent Effects. As described in a previous report,[24] formation of the NHC–CO_2 bond is accompanied by increasing zwitterionic character, which formally transfers charge from the heterocycle to the carboxylate group. Thus, increasing bonding is accompanied by an increasing dipole moment, and the stronger, shorter, and more polar bonds are stabilized in more polar solvents. In the case of **2**, a robust linear free energy relationship was found between the decarboxylation barrier ($\Delta G^{‡}$) and Reichardt's $E_T(30)$ solvent polarity scale. All of the derivatives examined here show the same relationships: the NHC–CO_2 bonds get stronger, shorter, and more polar in solvents of increasing polarity (Table 2). Three examples are shown in Figure 6, where the charge densities of compounds **2**, **10**, and **13** are illustrated as shaded

DOI: 10.1021/acs.joc.6b02755
J. Org. Chem. 2017, 82, 1552–1557

Table 2. $C_{NHC}-C_{CO2}$ Bond Distances (Å) for the 26 NHC–CO_2 Models in Various Solvents using the SMD Implicit Solvation Model

NHC–CO_2	gas	1,4-dioxane	acetonitrile	MeOH	water	Δ(gas–water)
1	1.552	1.544	1.533	1.518	1.515	0.037
2	1.576	1.568	1.541	1.530	1.522	0.054
3	1.570	1.559	1.544	1.529	1.526	0.044
4	1.569	1.562	1.549	1.531	1.529	0.040
5	1.564	1.553	1.554	1.540	1.538	0.026
6	1.581	1.566	1.550	1.528	1.525	0.056
7	1.568	1.562	1.553	1.541	1.539	0.029
8	1.598	1.580	1.562	1.542	1.538	0.060
9	1.579	1.566	1.548	1.523	1.520	0.059
10	1.604	1.586	1.564	1.542	1.539	0.065
11	1.592	1.574	1.559	1.540	1.537	0.055
12	1.615	1.592	1.568	1.550	1.546	0.069
13	1.579	1.563	1.547	1.528	1.523	0.056
14	1.579	1.568	1.553	1.534	1.532	0.047
15	1.590	1.576	1.562	1.544	1.541	0.049
16	1.613	1.583	1.560	1.540	1.537	0.076
17	1.585	1.569	1.555	1.542	1.539	0.046
18	1.565	1.553	1.541	1.527	1.526	0.039
19	1.553	1.541	1.524	1.505	1.501	0.052
20	1.567	1.556	1.542	1.527	1.524	0.043
21	1.503	1.497	1.492	1.490	1.488	0.015
22	1.590	1.581	1.568	1.553	1.549	0.041
23	1.592	1.576	1.561	1.546	1.542	0.050
24	1.582	1.568	1.553	1.537	1.532	0.050
25	1.570	1.565	1.558	1.545	1.540	0.030
26	1.584	1.570	1.558	1.543	1.540	0.044

isosurfaces of the molecular electrostatic potential where dark blue denotes positive charge and dark red shows negative charge.

The strong dependence of the NHC–CO_2 dissociation barrier on solvent polarity points to the possibility of developing catalytic systems that utilize this property to modulate capture of CO_2, which would be favored in polar media, and release of reduction products would presumably be favored in low-polarity media. For this reason, it is useful to identify rapid methods for predicting the sensitivity of a given NHC–CO_2 bond to changes in the solvent polarity. Intuitively it would be expected that NHC–CO_2 complexes that are weakly formed in the gas phase ought to be more readily stabilized by solvent polarity. In contrast, NHC–CO_2 complexes that are more fully formed in the gas phase ought to show less dependence on solvation. In this context, solvent dependence is defined as the absolute value of the slope of the best line relating bond distance (as a proxy for the free energy barrier) to the $E_T(30)$ value for various solvents (gas, 27.1; 1,4-dioxane, 36.0; MeCN, 45.6; MeOH, 55.4; H_2O, 63.1). These solvent dependence values are, in turn, compared to the gas-phase NHC–CO_2 bond distance, as illustrated in Figure 7.

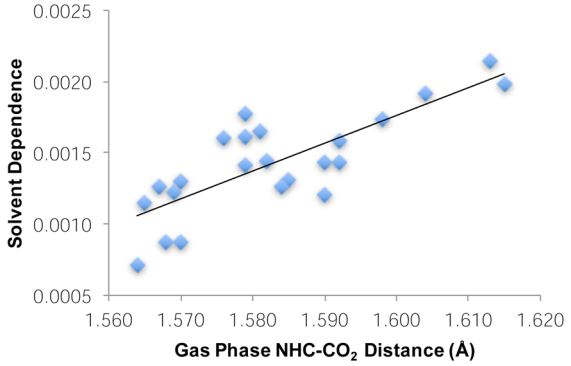

Figure 7. Solvent dependence (see text for explanation) of NHC–CO_2 bond distance increases with the gas-phase NHC–CO_2 distance.

Generally speaking, weakly bound complexes such as dinitro derivative **12** show a strong dependence on $E_T(30)$ and more tightly bound complexes, such as dimethyl derivative **6**, are less influenced by the solvent.

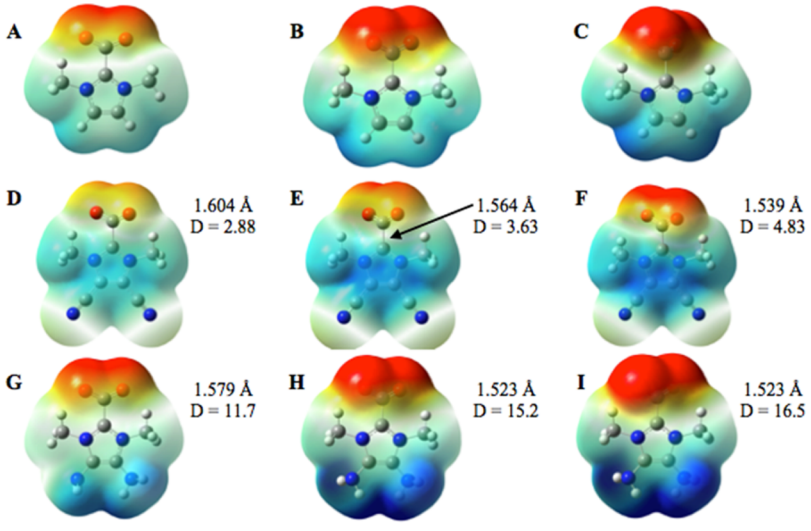

Figure 6. Structures derived from DFT optimizations using the SMD implicit solvation model on NHC–CO_2 **2** (A–C), **10** (D–F), and **13** (G–I) in the gas phase, acetonitrile, and water (left to right). The shaded isosurfaces are representations of the molecular electrostatic potential, where dark blue denotes positive charge density (+0.092 e/Å^3) and dark red denotes negative charge density (−0.092 e/Å^3). The bond length represents the $C_{NHC}-C_{CO2}$ calculated value, and the dipole moment (D) is also illustrated.

DOI: 10.1021/acs.joc.6b02755
J. Org. Chem. 2017, 82, 1552–1557

CONCLUSION

Herein we have described a computational approach to modeling the bond distances between 26 NHCs and carbon dioxide in the gas phase and four different solvents varying in polarity using the SMD implicit solvation model. The calculated bond distances differ greatly on going from nonpolar 1,4-dioxane to more polar H_2O as the bond shortens and favors the formation of NHC−CO_2. Both electronic and steric effects contribute to the lengthening or shortening of the bond, though a clear link between the two is not evident at this time. However, it appears that electronic effects contribute to a larger variance in bond distances when the solvent polarity is increased. For example, the degree of change in the bond distance for **5** on going from the gas phase to water is not as prominent that in the change for **8**−**10**, which have contributing electronic substituents, or that in compound **16**, which includes an oxygen heteroatom in the ring (Table 2). A large variance in bond length between nonpolar and polar solvents would be ideal for a CCS/CCU reagent, as it would be able to bind tightly to CO_2 in a polar solvent and be able to be released or recycled by simply switching to a more nonpolar medium. The computational results outlined above should provide an easy and efficient means for probing further development of heterocyclic 2-carboxylates for CO_2 capture and storage reagents or catalysts for the conversion of CO_2.

ASSOCIATED CONTENT

Supporting Information

The Supporting Information is available free of charge on the ACS Publications website at DOI: 10.1021/acs.joc.6b02755.

Cartesian coordinates and energies for the 26 NHC−CO_2 models, the transition states for the compounds in Table 1 and for **2** using the M11, M062X, and B3PW91 functionals, and a complete reference for the computational software used (PDF)

AUTHOR INFORMATION

Corresponding Author

*E-mail for D.E.F.: falvey@umd.edu.

ORCID

Derek M. Denning: 0000-0002-6804-4697

Notes

The authors declare no competing financial interest.

ACKNOWLEDGMENTS

We thank the Chemistry Division of the National Science Foundation for financial support.

REFERENCES

(1) Dlugokencky, E.; Tans, P. NOAA/ESRL (www.esrl.noaa.gov/gmd/ccgg/trends/).

(2) Markewitz, P.; Kuckshinrichs, W.; Leitner, W.; Linssen, J.; Zapp, P.; Bongartz, R.; Schreiber, A.; Müller, T. E. *Energy Environ. Sci.* **2012**, *5*, 7281−7305.

(3) Appel, A. M.; et al. *Chem. Rev.* **2013**, *113*, 6621−6658.

(4) Lu, W.; Sculley, J. P.; Yuan, D.; Krishna, R.; Wei, Z.; Zhou, H.-C. *Angew. Chem., Int. Ed.* **2012**, *51*, 7480−7484.

(5) Goeppert, A.; Czaun, M.; May, R. B.; Prakash, G. K. S.; Olah, G.; Narayanan, S. R. *J. Am. Chem. Soc.* **2011**, *133*, 20164−20167.

(6) Didas, S. A.; Choi, S.; Chaikittisilp, W.; Jones, C. W. *Acc. Chem. Res.* **2015**, *48*, 2680−2687.

(7) Darunte, L. A.; Oetomo, A. D.; Walton, K. S.; Sholl, D. S.; Jones, C. W. *ACS Sustainable Chem. Eng.* **2016**, *4*, 5761−5768.

(8) Pinto, A. M.; Rodriguez, H.; Colón, Y. J.; Arce, A., Jr; Arce, A.; Soto, A. *Ind. Eng. Chem. Res.* **2013**, *52*, 5975−5984.

(9) Mokhtarani, B.; Khatun, A. N.; Mafi, M.; Sharifi, A.; Mirzaei, M. *J. Chem. Eng. Data* **2016**, *61*, 1262−1269.

(10) Ménard, G.; Stephan, D. W. *J. Am. Chem. Soc.* **2010**, *132*, 1796−1797.

(11) Mömming, C. M.; Otten, E.; Kehr, G.; Fröhlick, R.; Grimme, S.; Stephan, D. W.; Erker, G. *Angew. Chem., Int. Ed.* **2009**, *48*, 6643−6646.

(12) Sumida, K.; Rogow, D. L.; Mason, J. A.; McDonald, T. M.; Block, E. D.; Herm, Z. R.; Bae, T.-H.; Long, J. R. *Chem. Rev.* **2012**, *112*, 724−781.

(13) Tamura, M.; Honda, M.; Nakagawa, Y.; Tomishige, K. *J. Chem. Technol. Biotechnol.* **2014**, *89*, 19−33.

(14) Castro-Osma, J. A.; Lamb, K. J.; North, M. *ACS Catal.* **2016**, *6*, 5012−5025.

(15) Tlili, A.; Frogneux, X.; Blondiaux, E.; Cantat, T. *Angew. Chem., Int. Ed.* **2014**, *53*, 2543−2545.

(16) Tlili, A.; Blondiaux, E.; Frogneux, X.; Cantat, T. *Green Chem.* **2015**, *17*, 157−168.

(17) He, C.; Tian, G.; Liu, Z.; Feng, S. *Org. Lett.* **2010**, *12*, 649−651.

(18) Zhang, S.; Kang, P.; Meyer, T. J. *J. Am. Chem. Soc.* **2014**, *136*, 1734−1737.

(19) Lu, Q.; Rosen, J.; Zhou, Y.; Hutchings, G. S.; Kimmel, Y. C.; Chen, J. G.; Jiao, F. *Nat. Commun.* **2014**, *5*, 3242.

(20) Kayaki, Y.; Yamamoto, M.; Ikariya, T. *Angew. Chem., Int. Ed.* **2009**, *48*, 4194−4197.

(21) Voutchkova, A. M.; Appelhans, L. H.; Chianese, A. R.; Crabtree, R. H. *J. Am. Chem. Soc.* **2005**, *127*, 17624−17625.

(22) Kayaki, Y.; Yamamoto, M.; Ikariya, T. *Angew. Chem.* **2009**, *121*, 4258−4261.

(23) Ajitha, M. J.; Suresh, C. H. *J. Org. Chem.* **2012**, *77*, 1087−1094.

(24) Denning, D. M.; Falvey, D. E. *J. Org. Chem.* **2014**, *79*, 4293−4299.

(25) Van Ausdall, B. R.; Poth, N. F.; Kincaid, V. A.; Arif, A. M.; Louie, J. *J. Org. Chem.* **2011**, *76*, 8413−8420.

(26) Dimroth, K.; Reichardt, C.; Siepmann, T.; Bohlmann, F. *Liebigs Ann. Chem.* **1963**, *661*, 1−37.

(27) Reichardt, C. *Liebigs Ann. Chem.* **1971**, *752*, 64−67.

(28) Denning, D. M.; Thum, M. D.; Falvey, D. E. *Org. Lett.* **2015**, *17*, 4152−4155.

(29) See the Supporting Information for the complete reference.

(30) Becke, A. D. *J. Chem. Phys.* **1993**, *98*, 1372−1377.

(31) Lee, C.; Yang, W.; Parr, R. G. *Phys. Rev. B: Condens. Matter Mater. Phys.* **1988**, *37*, 785−789.

(32) Marenich, A. V.; Cramer, C. J.; Truhlar, D. G. *J. Phys. Chem. B* **2009**, *113*, 6378−6396.

(33) Peverati, R.; Truhlar, D. G. *J. Phys. Chem. Lett.* **2011**, *2*, 2810−2817.

(34) Zhao, Y.; Truhlar, D. G. *Theor. Chem. Acc.* **2008**, *120*, 215−241.

(35) Perdew, J. P.; Wang, Y. *Phys. Rev. B: Condens. Matter Mater. Phys.* **1992**, *45*, 13244−13249.

(36) Craig, N. C.; Groner, P.; McKean, D. C. *J. Phys. Chem. A* **2006**, *110*, 7461−7469.

(37) Van Ausdall, B. R.; Glass, J. L.; Wiggins, K. M.; Aarif, A. M.; Louie, J. *J. Org. Chem.* **2009**, *74*, 7935−7942.

(38) Hammett, L. P. *J. Am. Chem. Soc.* **1937**, *59*, 96−103.

DOI: 10.1021/acs.joc.6b02755
J. Org. Chem. 2017, 82, 1552−1557